Digital Subcarrier Multiplexing: Enabling Software-Configurable Optical Networks

Dave Welch, *Fellow, IEEE*, Antonio Napoli, Johan Bäck, Sanketh Buggaveeti, Carlos Castro, Aaron Chase, Xi Chen, Vince Dominic, Thomas Duthel, Tobias A. Eriksson, Sezer Erkilinç, Peter Evans, Chris R. S. Fludger, Ben Foo, Thomas Frost, Paul Gavrilovic, Steven J. Hand, Aditya Kakkar, Ales Kumpera, Vikrant Lal, *Member, IEEE*, Robert Maher, Fabio Marques, Fady Masoud, Atul Mathur, *Member, IEEE*, Ray Milano, *Member, IEEE*, Miguel Iglesias Olmedo, Magnus Olson, Don Pavinski, João Pedro, *Senior Member, IEEE*, Amir Rashidinejad, Parmijit Samra, Warren Sande, Azmina Somani, Han Sun, Norman Swenson, *Senior Member, IEEE*, Huan-Shang Tsai, Amin Yekani, Jiaming Zhang, and Mehrdad Ziari, *Member, IEEE*

(Invited Paper)

***Abstract*—The various topologies, traffic patterns and cost targets of optical networks have prevented the deployment of end-to-end solutions across multi-domains, and the optimization of the network as a whole. The consequent limitations in flexibility, scalability, and adaptability of optical networks will become increasingly important with new applications, such as 5G/6G. Coherent transceivers based on digital subcarrier multiplexing (DSCM) are proposed to address these current constraints. In particular, DSCM allows (i) the design of high-capacity point-to-point (P2P) and -multipoint (P2MP) optical networks; (ii) simplified aggregation with passive optics; and (iii) connections between low- and high-speed transceivers. Furthermore, DSCM-based networks reduce the number of opto-electro-opto stages, halve the number of bookended transceivers, and provide a better match for existing hub-and-spoke (H&S) traffic patterns in fast-growing and dynamic access/metro segments. A DSCM-based transceiver will pave the way for the deployment of next-generation flexible, adaptable, and scalable software-configurable optical networks. Key steps and elements to realize this solution are laid out, and promising applications outlined. The first real-time experimental results of coherent P2MP transceivers are presented.**

***Index Terms*—Digital subcarrier multiplexing, point-to-multipoint, coherent access, metro aggregation, fronthaul, 5G.**

Manuscript received 13 July 2022; revised 14 September 2022; accepted 23 September 2022. Date of publication 3 October 2022; date of current version 16 February 2023. *(Corresponding author: Antonio Napoli.)*

Dave Welch, Sanketh Buggaveeti, Aaron Chase, Vince Dominic, Peter Evans, Ben Foo, Thomas Frost, Paul Gavrilovic, Steven J. Hand, Vikrant Lal, Robert Maher, Atul Mathur, Ray Milano, Miguel Iglesias Olmedo, Parmijit Samra, Warren Sande, Norman Swenson, Huan-Shang Tsai, and Mehrdad Ziari are with the Infinera Corporation, 6373 San Ignacio Avenue, San Jose, CA 95119 USA (e-mail: dwelch@infinera.com; SBuggaveeti@infinera.com; achase@infinera.com; vdominic@infinera.com; pevans@infinera.com; bfoo@infinera.com; tfrost@infinera.com; pGavrilovic@infinera.com; shand@infinera.com; vlal@infinera.com; rmaher@infinera.com; aMathur@infinera.com; rMilano@infinera.com; molmedo@infinera.com; psamra@infinera.com; wsande@infinera.com; nswenson@infinera.com; ctsai@infinera.com; mziari@infinera.com).

Antonio Napoli, Carlos Castro, Thomas Duthel, and Chris R. S. Fludger are with the Infinera, 81541 Munich, Germany (e-mail: anapoli@infinera.com; cacastro@infinera.com; tduthel@infinera.com; cfludger@infinera.com).

Johan Bäck, Xi Chen, Tobias A. Eriksson, Sezer Erkilinç, and Magnus Olson are with the Infinera, 117 43 Stockholm, Sweden (e-mail: jbaeck@infinera.com; xi.chen@infinera.com; teriksson@infinera.com; serkilinc@infinera.com; molson@infinera.com).

Fabio Marques and João Pedro are with the Infinera Unipessoal Lda, 2790-078 Carnaxide, Portugal (e-mail: famarques@infinera.com; jpedro@infinera.com).

Aditya Kakkar, Ales Kumpera, Fady Masoud, Amir Rashidinejad, Azmina Somani, Han Sun, and Amin Yekani are with the Infinera, Ottawa K2K 2X3, Canada (e-mail: aKakkar@infinera.com; akumpera@infinera.com; fMasoud@infinera.com; arashidinejad@infinera.com; asomani@infinera.com; hsun@infinera.com; ayekani@infinera.com).

Don Pavinski and Jiaming Zhang are with the Infinera Corporation, 6373 San Ignacio Avenue, San Jose, CA 95119 USA, and also with the Infinera Corporation, Allentown, PA 18106 USA (e-mail: dpavinski@infinera.com; JiZhang@infinera.com).

Color versions of one or more figures in this article are available at https://doi.org/10.1109/JLT.2022.3211466.

Digital Object Identifier 10.1109/JLT.2022.3211466

I. Introduction

INTERNET connectivity underpins countless services that shape our daily lives, fueling the exponential growth of global IP data traffic [1]. It is hard to imagine the current IT-based society without fiber optics and its relentless technological evolution that has allowed Content Service Providers (CSPs) to meet the growing demand for capacity with flat budgets.

For example, the evolution of optical transport throughput in Dense Wavelength Division Multiplexing (DWDM), from 2000 to today, has been remarkable, with an 80× increase — from 10 Gb/s/λ [2], [3] to 800 Gb/s/λ [4], [5]. This increase led to drastic reductions in the Cost per Transported Bit (CpB), through improvements in components and Digital Signal Processing (DSP), which allowed higher-order modulation formats to be exploited for increased Spectral Efficiency (SE) and fiber capacity [6]. However, this strategy is now saturating and provides only incremental reductions in CpB as we approach the Shannon capacity limit [7, Fig. 2], and new solutions are required. Several proposals have been made, including multi-band transmission [8], [9], multi-core/-mode fibers [10], and hollow-core fibers [11]. These solutions are not mature and the last two also require significant investments in fiber infrastructures. Each

of these approaches seeks to enable more fiber capacity by increasing the available spectrum.

At the same time, there is an industry push to transform coherent transceivers in the form of pluggable modules. Although this does not increase the total fiber throughput, it has the promise of reducing the cost per unit of deployed capacity. To this end, initiatives such as 400ZR [12] have been developed. This solution is being adopted by hyperscalers for metro applications, e.g., Data Center Interconnect (DCI), and is being considered by numerous CSPs also for metro core networks [13].

Another approach is to look at how networks are built and identify sources of inefficiency. A particular area that has been studied is the way CSP metro and access networks are deployed using Point-to-Point (P2P) transceivers of different rates, interconnected by a hierarchy of routers or other intermediate aggregation devices that are used to minimize the Total Cost of Ownership (TCO) by optimizing the capacity of transceivers existing on any given link. Larger transceivers are typically less expensive per unit of capacity, but deploying more capacity than required is costly and spectrally inefficient [14].

Moreover, in the fastest growing network segments, access and metro, traffic patterns are mainly Hub-and-Spoke (H&S)[1] and highly dynamic [15]. Here, a multitude of low-speed transceivers (end users) are connected to a few high-speed transceivers (hubs). In this scenario, the aforementioned P2P types of connections are suboptimal, and the possibility of enabling low to high speed transceiver communication with a Point-to-Multipoint (P2MP) solution — as shown in [7, Fig. 1] — would significantly simplify network design, planning, and management.

P2MP is not a new concept, having been used in wireless systems [16] and in commercial deployments in fiber optics, in Passive Optical Network (PON) [17], which enabled the successful wide deployment of the broadband internet at home. However, future innovation, for example, 5G/6G, will require capacity that cannot be provided by existing Intensity Modulation Direct-Detection (IM-DD) solutions [18] and it will be necessary to move towards a coherent solution in access/metro [7], [19]. To solve the above issues, we propose to realize P2MP DWDM with coherent technology. Among the options available for the design of the transceiver, the following are the most relevant: Sliceable Bandwidth Variable Transponder (S-BVT) [20], Orthogonal Frequency-Division Multiplexing (OFDM) [21], and Digital Subcarrier Multiplexing (DSCM) [7]. Among them, we select DSCM-based transceivers, which represent a sweet spot in terms of hardware and enabled applications. For example, with respect to S-BVT, DSCM requires only one laser, and compared to OFDM, it provides a better tolerance to time-frequency synchronization within the DSP algorithms. This is because OFDM uses a significantly lower symbol rate, making the detection of Subcarriers (SCs) complex, especially when arriving from different OFDM transmitters at different distances.

The use of DSCM was initially pursued for its propagation advantages [4], [22], [23], [24], [25], [26], [27], particularly for long-haul transmission. Here, however, we are proposing it to efficiently realize P2MP coherent transceivers that can enable software-configurable P2MP optical networks [7]. For instance, this type of transceivers can be advantageously used in aggregation networks, characterized by a H&S traffic pattern between smaller leaf nodes and larger hub nodes. Here, DSCM creates independent channels, called SCs that act as virtual channels that can be managed by the Software Defined Networking (SDN) controller. The SCs can be transmitted in P2P or P2MP system configuration, paving the way for a low cost design of optical networks. Electronic aggregation layers can now be replaced by passive optics, and H&S traffic patterns can be transported more efficiently through SCs. The larger transceivers can then be deployed at the hub nodes, and lower capacity transceivers at the leaf sites, resulting in fewer transceivers deployed and greater flexibility in managing the capacity of highly dynamic traffic patterns [28]. Equally important, fewer and larger ports are allowed on hosting devices, and active aggregation equipment, such as leaf switches or aggregation routers, can be removed from the network architecture [29]. The result is a substantial reduction in network costs.

Finally, with the possibility of fine-tuning the spectrum, DSCM-based software-configurable optical networks can enable Bandwidth (BW) allocation on demand when and where needed, mimicking statistical multiplexing [30].

The novelty of this approach lies in increased flexibility, scalability, and ease of upgrading. In fact, while DWDM and Time Division Multiple Access (TDMA) PON allow a passive combination of $>$100G and of $\geq$1G channels, respectively, DSCM can dynamically aggregate tens and hundreds of Gb/s. Furthermore, DSCM can optimize the spectrum and maximize transmission performance in the case of a cascade of Reconfigurable Optical Add and Drop Multiplexers (ROADM) [31].

We foresee that the universal applicability of this technology[2] – from access to long-haul – will enable economies of scale in the manufacture of Application-specific Integrated Circuits (ASIC) and optical modules. The realization of pluggables with higher performance with smaller form factors was challenged by the complexity of the optics, the need for amplification of light with a fiber amplifier, and the size and power consumption of the DSP chips. These challenges are being mitigated through advances in photonic technology and by Complementary Metal-oxide-semiconductor (CMOS) technology with 7 nm and beyond to support higher density and lower power consumption.

The application of DSCM-based P2MP networks has already been evaluated in several techno-economic studies [29], [33], and has been experimentally validated in laboratory experiments [7] and trials [34]. These investigations have shown the potential for 400G transmission over existing PONs. In these scenarios, significant cost reduction has been reported in [33], by eliminating the need for routing [29] or reducing Opto-Electro-Optical (OEO) conversions [7]. In this paper, for the first time, we present experimental results with passive optical aggregation and with signals transmitted and received by a real-time DSCM-based P2MP system operating at 100G/200G/400G. Herein, we

[1]The terminology Hub-and-Spoke will be used interchangeably with Hub-and-Leaf throughout the text

[2]We refer to the proposed technology as the one that can be employed throughout the entire network by using the same material and transmission technique and that will consequently reduce the amount of processing in the network [32].

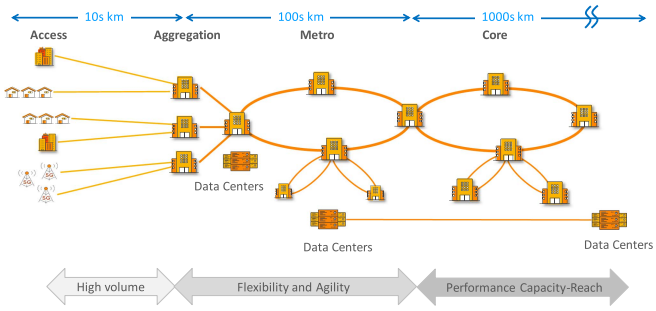

Fig. 1. Generic topology of a telecommunication network with the three main segments: access, metro, and core.

analyze various configurations, and measure real-time error-free transmission. The remainder of this work is divided as follows. In Section II we present the State-of-the-Art (SotA) and describe a solution based on DSCM for software-configurable optical networks. Benefits and challenges are discussed along with the key-building blocks. Section III shows the potential advantages of Intelligent Pluggable Transceivers (IPTs) when used as a universal element throughout the network [32]. In particular, Transmitter-Receiver Optical Sub-Assembly (TROSA), DSP, and the intelligent features enabled by the DSCM pluggables are discussed in detail. Section IV explains the management and control plane in DSCM-based software-configurable optical networks. Topics such as SC management and channel discovery are also explored. Section V discusses how the need for industrial processes — focusing on high-volume products in optics — is a key part of the proposed solution. Section VI presents multiple applications of this new technology, by techno-economically comparing it with the SotA to show the benefit of the proposed approach. Section VII presents the first experimental results for 100G/200G/400G coherent P2MP transceiver prototypes on our Evaluation Boards (EVBs) platform in a Back-to-Back (B2B) configuration, while performing optical aggregation and broadcast. Finally, Section VIII examines the need for a healthy supply chain and an ecosystem that could be established through Multi-Source Agreements (MSAs). Lastly, Section IX summarizes the article.

II. Towards Software Configurable Optical Networks

In this section, we discuss the SotA (Section II-A); the innovation and key elements needed to build software-configurable optical networks (Secs. II-B and II-C); and the main benefits of this solution (Section II-D).

A. State-of-The-Art

Fig. 1 illustrates a simplified telecommunication network from access to the core. Distances between links, network topologies, traffic growth, technology, hardware, and innovation are different in individual segments of the network, due to users, density, and geography, as summarized in Table I.

a) Distances and topologies: Connections range from tens of kilometers (access), up to 250 km (metro) and >1000 km (core). Typical topologies are trees and horseshoes (access/metro) and rings (metro/core) [7].

TABLE I
Challenges and Characteristics of the Considered Three Network Segments

	Access	Metro	Core
Traffic growth	high	high	moderate
Technology	IM-DD [35]	coherent, 400G/λ [12]	coherent, 800G/λ [4]
Hardware requirements	high volume low power	flexibility	performance
Innovation	slow	fast	fast

b) Traffic growth: A large number of end users have access to the broadband Internet [35]. For this reason, Internet Protocol (IP) annual data traffic sees an increase of 60% in access/metro and 30% in metro/core [1]. Connections from low-speed to high-speed network domains are realized through electronic aggregation at the access/metro and metro/core nodes. Traffic patterns originate mainly from P2MP configurations (H&S patterns) in access/metro, and from P2P configurations in metro/core.

c) Technology and hardware requirements: Due to the large number of users in access/metro, the main criteria for wide deployment and operational success are low power consumption and high-volume production of the transceivers. Standards are required to guarantee multivendor interoperability [36], with the drawback of delaying the adoption of new technologies. However, in core networks, high-end performance is mandatory [4], [37] and standards have not been established.

d) Innovation: In access, existing standards provide a capacity of up to 1G per user [38]. This scenario is expected to change with the introduction of 5G/6G and Virtual and Augmented Reality (VR/AR). Next-generation access PON will support up to IM-DD 50G with Time Division Multiplexing (TDM) [36], [39] and 100G with flexible-rate achieved using flexible modulation format, and FEC code rate [40]. In 100G coherent outlook PON [41], both TDM and Frequency Division Multiplexing (FDM) are being considered in [19], instead of FDM only for PON overlay, 5G front-haul and metro aggregation, etc., as proposed in [7], [34], [42], [43]. In metro and for DCI, coherent-based approaches such as 400ZR [12] are being deployed. Finally, in the core network, traffic is further aggregated to be transported over long-haul links. Here, innovation is faster, with the data rate per card doubling every 3–4 years [44].

B. Realizing Software-Configurable Optical Networks

In software-configurable optical networks, services are dynamically adapted through SDN. By adopting coherent P2MP technology, we can increase the level of simplification, flexibility, and scalability of existing networks. In addition, this approach enables multi-generational networks, while preserving the optical link performance. We envision a densely interconnected network where a large number of low-cost transceivers communicate among them, at different rates, to support H&S traffic patterns. Fig. 2 illustrates an example of a possible future network. Here, several low-speed transceivers — exhibiting a series of virtualized transport functions — are connected to the Optical Line System (OLS). The transceivers can connect

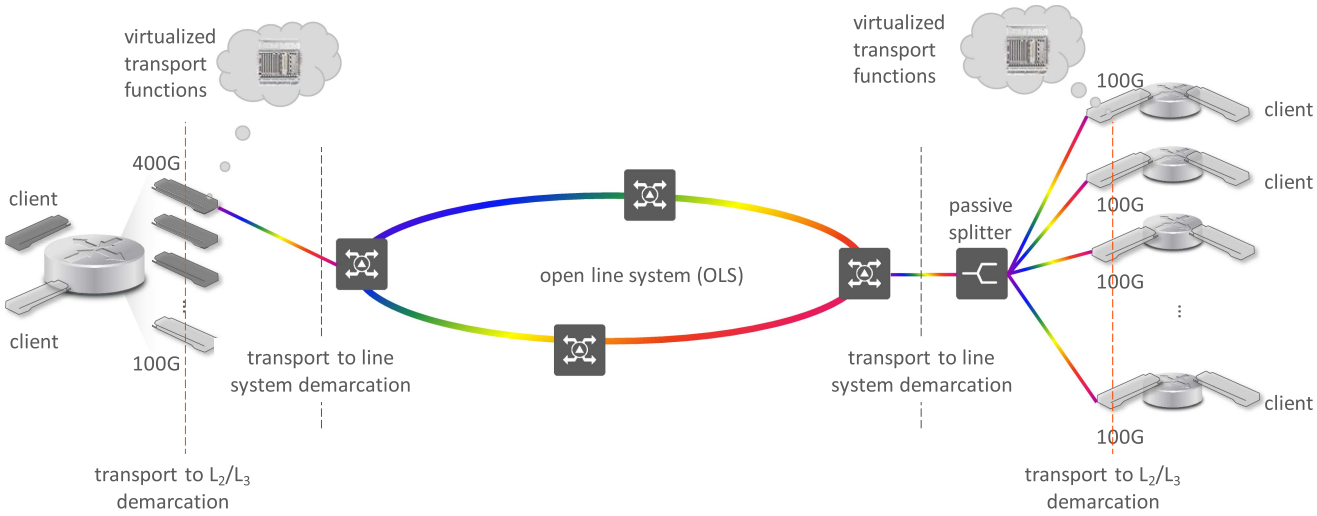

Fig. 2. Software-configurable optical network and its impact on modern optical networks.

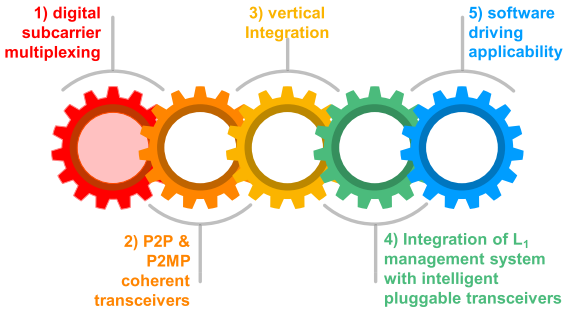

Fig. 3. The five key elements of software-configurable optical networks. DSCM (in red) is the "engine".

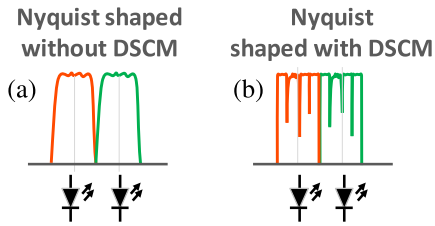

Fig. 4. Qualitative comparison of Nyquist-shaped dual-λ channel (a) without and (b) with DSCM.

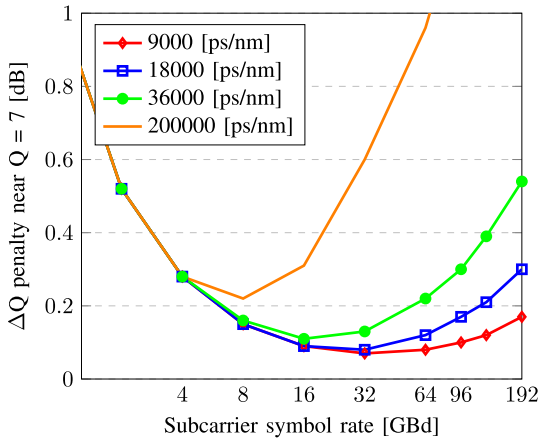

Fig. 5. Q penalty in [dB] versus symbol rate as function of D_{acc} for laser with Linewidth (LW) = 100 kHz.

seamlessly to the network through passive splitter aggregation, as shown in the right of Fig. 2, thus eliminating the need for OEO conversion and reducing the number of bookended transceivers. In addition to cost savings, this improves the environmental footprint and reduces power consumption. Furthermore, with dynamic bandwidth allocation, the spectrum will be used more efficiently, as demonstrated in [14].

C. The Key Elements of Software-Configurable Optical Networks

Software-configurable optical networks require the coexistence of the following elements: (i) DSCM, (ii) P2P and P2MP coherent transceivers, (iii) vertical photonic integration, (iv) integration of the L_1 management system with IPTs, and (v) software driving applications. Among these, DSCM is the "engine," as it provides the main added value when compared to traditional solutions, as visualized in Fig. 3.

1) Digital Subcarrier Multiplexing: DSCM [45], [46] differs from OFDM because SCs are not orthogonal, and each SC carries a significantly higher symbol rate. DSCM has been used in commercial transponders for metro/core markets up to transoceanic distances with symbol rates above >10 GBd and up to 8 SCs, achieving data rates of 800G [4], [47]. Figure 4 illustrates a qualitative comparison between a Nyquist-shaped dual-λ channel (a) without and (b) with DSCM. To date, DSCM has been used mainly for its high tolerance to propagation impairments and/or to simplify and improve the design of DSP algorithms [4]. For example, DSCM (i) presents a high tolerance to Enhanced Equalization Phase Noise (EEPN), which is relevant for transoceanic links, since the enormous amount of Accumulated Dispersion (D_{acc}) causes the laser phase noise not to be constant in the time range of the D_{acc}, as shown in [4, Fig. 1, 2]; (ii) enables granular optimization of the symbol rate per SC as a function of D_{acc} (see Fig. 5); (iii) allows adaptation of the spectrum to filter cascades [31], [48]; (iv) has a better nonlinear

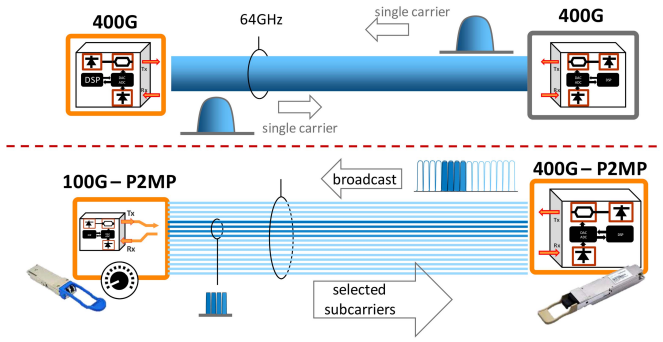

Fig. 6. Comparison between (a) single-carrier and (b) DSCM-based transceivers.

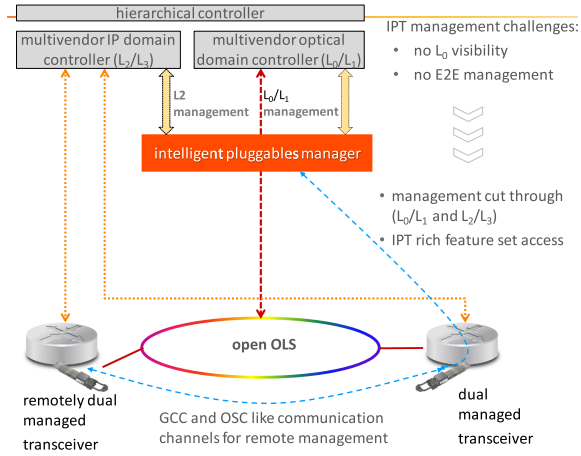

Fig. 7. Integration of L_1 management system with IPTs.

tolerance compared with the single-carrier counterpart [26], [27], [49].

In addition to the characteristics mentioned above, the DSCM hub generates SCs using only one laser. Thanks to this approach, the SCs in the downlink/broadcast direction can be positioned very closely to each other with minimal gap in between as reported in Section III-B and in Fig. 13. Furthermore, in the uplink/aggregation direction, by leveraging DSP-aided wave-locking to the hub spectrum, different leaf nodes can also be placed very tightly next to each other. This tight channel spacing can only be achieved with P2MP and digital SCs. An implementation on P2P networks or based on individual laser sources – per carrier – would not only be much more costly, but would also require significantly wider guard bands between SCs to allow for frequency fluctuations of the lasers. Section III-B discusses this in more detail. Finally, the SCs can be managed and controlled as independent channels, providing architectural benefits for the realization of P2MP optical networks with increased levels of flexibility.

2) Point-to-Point and Point-to-Multipoint Coherent Transceivers: The main difference between a P2P and a P2MP transceiver lies in the ability of the latter to establish communication between two transceivers that transmit at different speeds. This is visually described in Fig. 6, where in Fig. 6(a) an optical connection is established between two P2P transceivers, each at 400G with a BW occupancy of 64 GHz. This transceiver uses a single-carrier configuration. On the other hand, Fig. 6(b) represents a P2MP connection, where two transceivers — at two different data rates and with different pluggable form factors — communicate using DSCM with a granularity of 25Gb/s. In both cases, we consider the transmission of coherent 16 Quadrature Amplitude Modulation (16-QAM) with dual polarization, and the gross symbol rate of 64 GBd and of 4 GBd, for single-carrier and DSCM, respectively. P2MP provides some clear benefits. For example, the 400G P2MP DSCM-based transceiver can broadcast optical channels to multiple passively coupled receivers (similarly to wireless systems), as shown in Fig. 6(b). Here, up to 16 receivers can each receive one SC from the hub. Furthermore, the joint availability of SC and P2MP results in additional flexibility and benefits compared to traditional P2P transceivers: when connected to a router or any host card, a P2MP transceiver will occupy the same hardware slot as a traditional P2P transceiver, but it allows one to dynamically configure multiple optical channels in steps of 25Gb/s.

3) Vertical Photonic Integration: Indium Phosphide (InP) Photonic Integrated Circuit (PIC) technology is particularly suitable for the application we are envisioning [50]. A single, widely tunable laser is needed to supply light for high-speed coherent DSCM transmission, and it is also needed as a local oscillator for coherent detection. In leaf mode, the DSP in the receiver locks the transceiver PIC's shared Transmitter (TX)/Receiver (RX) laser to the incoming signal used for transmission. Integrated Semiconductor Optical Amplifiers (SOAs) enable compensation for modulation, splitting, and other losses to ensure signal integrity and 0 dBm output power.

4) Integration of L_1 Management System With Intelligent Pluggable Transceivers: The envisioned network will be more flexible than a traditional P2P network and will therefore benefit from a higher level of "softwarization" and self-management. For example, transceivers will be able to adapt their traffic to variable needs, based on the optimization of different cost functions. It will also be possible for them to use the information from an embedded Optical Spectrum Analyzer (OSA) to remotely troubleshoot the interaction of SCs with the OLS. Fig. 7 shows an example of the management of such a network, with two dual-managed transceivers connected to an OLS. Here, the Intelligent Pluggable Manager (IPM) enables the management of the network by the hierarchical controller, which orchestrates management through two multi-vendor IP domain controllers: one controller for L_0/L_1 and the OLS, and one for L_2/L_3. System-level communication is carried out using remote management channels, such as General Communication Channel (GCC) and Optical Service Channel (OSC). Compared to a traditional network, IPTs provide a wide range of features that can improve the performance and operations of virtualized transport functions on a variety of host devices and optical systems. The range of these features includes remote management, topology and BW discovery and management, far-end transport demarcation, bidirectional single-fiber transmission, restoration, advanced optical diagnostics, and telemetry streaming.

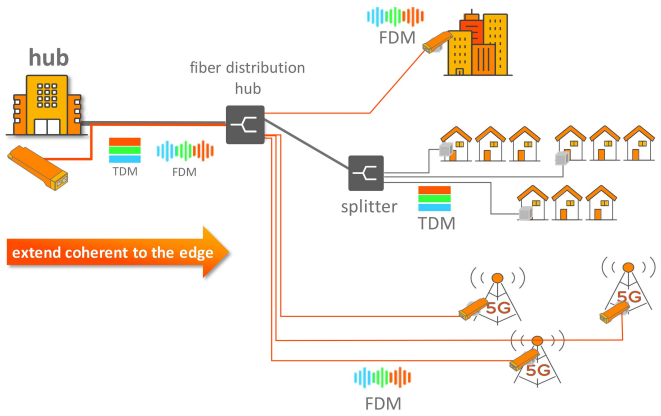

Fig. 8. Software-driven applications with DSCM-based P2MP optical networks: (a) hub; (b) PON overlay; (c) traditional PON infrastructure; (d) 100G/400G 5G front-haul.

5) Software-Driven Applications: Software-configurable optical networks enable a more efficient use of existing telecommunication infrastructure and bring ultra-high capacity to a series of applications, e.g., PON overlay and 5G front-haul. Figure 8 shows some applications enabled by a IPT on the same PON infrastructure. In the scenarios considered, a 400G DSCM-based P2MP coherent transceiver at the hub allows the following use cases:

- PON overlay: The PON overlay achieves an 8× increase in capacity, i.e., 400G coherent over PON [7], [34] with respect to the most advanced (but not yet deployed) IM-DD solution [51].
- Ultra-high capacity front-haul: The upcoming demand for ultra-high capacity front-haul can be efficiently and flexibly met with scalable DSCM-based P2MP. This allows scaling of capacity as needed over time.
- More efficient use of different network types and topologies, such as horseshoes, stars, trees, and rings. (Figure 8 shows an example of a tree.)

D. Benefits of Software-Configurable Networks

Software-configurable networks represent a paradigm shift in the current way of designing and managing optical systems. In the following, we list a series of benefits obtained with DSCM-based P2MP transceivers.

a) Reach versus power: Modern coherent transceivers are software-configurable and can deliver the required capacity on a given fiber link while, e.g., minimizing power consumption. The reach is affected by changes, among others, in the optical output power and the strength of the Forward Error Correction (FEC) scheme used. The introduction of DSCM unlocks an additional degree of freedom in terms of system planning and optimization.

b) Point-to-point versus Point-to-multipoint: Legacy P2P transceivers are dedicated to a particular destination, and if a node is serving traffic to several other nodes (e.g., in a H&S traffic pattern), then a large number of smaller transceivers are required. Using DSCM-based P2MP transceivers, a single high-capacity transceiver can be deployed to serve multiple end points. This enables the capacity to be dynamically moved between end points, which, in turn, can be used to better match time-dependent traffic patterns and to allow the use of larger capacity transceivers with lower CpB.

c) Management via Host or Independent: Optical transceivers are typically managed by the controller on the host in which the transceiver is installed. This requires the host vendor to understand the details of DWDM technology and implement new features as the transceiver technology evolves. The introduction of coherent technology in pluggable transceivers places a severe strain on this model, as host vendors have to implement ever-changing updates to the DWDM transceiver information models. Furthermore, it also requires host vendors to support communication with transport layer network management systems. Advancements in CMOS technology reduce the size of features and reduce the power consumption in each new silicon node. This can be used to add more features to the transceiver ASIC, such as a Central Processing Unit (CPU) and memory to allow the use of a lightweight Operating System (OS), effectively allowing it to be a standalone network element, managed independently by an application communicating through the host, rather than being managed by the host itself. Independent management enables the use of a coherent transceiver in any device that requires high-capacity fiber connectivity and hides the complexity of optical transmission to its host. This model has been successfully used in Radio Access Network (RAN), where devices such as smart water meters or robotic lawnmowers can use a 5G chipset and a SIM card and receive wireless connectivity without knowing which cell tower they are connected to, neither the modulation format nor the carrier frequency. Similarly, we envision future optical networks with coherent transceivers deployed in a multitude of different hosts to support End-to-End (E2E) management while simultaneously presenting a very simple interface to the host devices.

d) Standards Compatibility: Next generation coherent transceivers will operate within an ecosystem of host devices using a shared fiber infrastructure to deliver high-capacity connectivity. There is a need for general industry agreement on form, fit, and function, in the form of MSAs or standards, to enable and accelerate the proliferation of next-generation transport networks.

e) Future proof upgrades: Additionally, DSCM-based transceivers enable a consistent and multi-generational network architecture based on a common "currency," where both the hub and the leaf node share the same building blocks: increments of 25Gb/s. This allows them to be upgraded to a new generation of modules independently. For example, hub sites can be seamlessly upgraded to 800 G without the need to upgrade any leaf nodes — something that is not possible for existing PONs — thus decoupling nodal upgrades from network-wide upgrades. In this way, network operators can maximize Return on Investment (ROI), ensure a smooth and cost-effective deployment of new technology in the network, and reduce Operational Expenditure (OPEX) with the flexibility introduced in terms of maintenance and operation.

f) Single fiber or dual fiber: Full duplex optical transmission on single-fiber infrastructures normally requires different

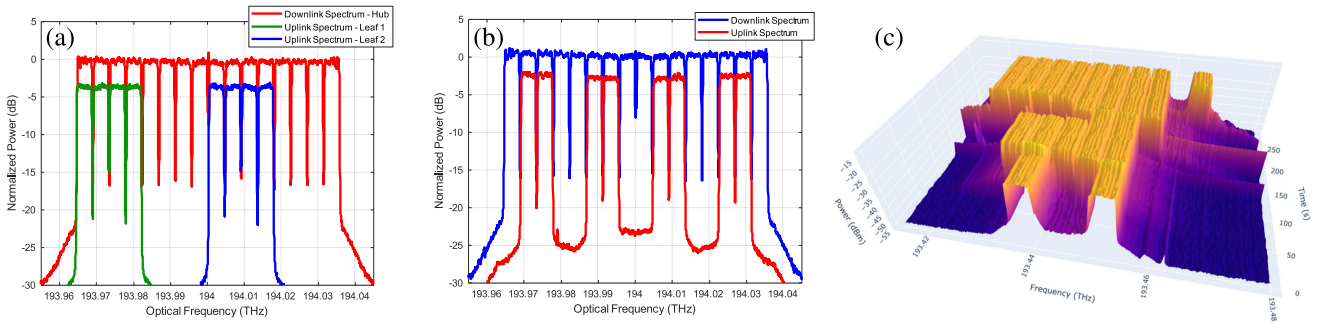

Fig. 9. Real-time Power Spectral Density (PSD) measurements of SCs: (a) 2×100G leaf nodes (green and blue) received by a 400G hub (red); (b) 4×50 G leaf nodes (red), received simultaneously by a 400G hub (blue); (c) SCs evolution vs time for dynamic bandwidth allocation.

wavelengths to be used for east- and west-bound traffic. Although this does not introduce any additional complexity for a IM-DD transceiver — photo detectors are wide-band receivers — a coherent transceiver requires a second laser for the local oscillator. This has implications for cost, space, and power and may not be feasible to implement within the specifications of a given form factor. DSCM is an elegant way to provide single-fiber interworking by using different subcarriers for east- and west-bound traffic. The capacity per direction can even be adapted to traffic loads, by choosing how many subcarriers to use per direction.

This provides significant benefits in applications where the cost of fiber is a significant part of the TCO, such as in access networks where the capacity per fiber is relatively low. It enables DSCM transceivers to be deployed in PON overlay applications, providing a step function in capacity compared to today's Gigabit Ethernet Passive Optical Network (GPON) and XGS-PON transceivers.

g) Variable spectral width for various ROADMs: Over the years, the International Telecommunication Union (ITU) has standardized a series of different DWDM channel plans, which have been developed by optical vendors and deployed by network operators. As symbol rates have increased, operators face the challenge of upgrading legacy line systems, as older add/drop multiplexers and ROADMs are too narrow spectrally to support modern coherent transceivers. To mitigate this, coherent transceivers support lower symbol rates to allow deployment on legacy line systems, e.g., a 60 GBd transceiver may have a 30 GBd mode.

A natural benefit of an optical transceiver based on DSCM is the ability to fine-tune the net symbol rate by selectively turning the digital SCs on & off. A 400Gb/s DSCM transceiver with 16-QAM SCs can be tuned in 4 GBd steps, providing unprecedented granularity and even allowing configurations where a single transceiver uses two adjacent fixed-grid channels for transmission. This can be very useful for maximizing the capacity and extending the service life of a legacy optical line system.

h) Re-allocation of bandwidth: This is one of the main properties of software-configurable optical networks, which provides a more efficient utilization of the spectrum by optimally allocating the SCs [14], [30]. This could also be done to maximize performance as a function of reach, channel, capacity, and/or power consumption. The real-time adaptation through an Application Programming Interface (API) could be exploited to deal with instantaneous channel variations, as shown in [30], or by optimizing SCs for narrow filtering [31], [48]. Such a network — based on the 4 GHz spectral granularity (25Gb/s capacity granularity) — can be managed with zero-touch, for example, in terms of on-demand activation or deactivation of the SCs.

Fig. 9(a)–(c) depicts a real-time evolution of the number of SCs that emulate real scenarios. In Fig. 9(a)–(b), we illustrate the spectra of two configurations with different types of leaf nodes, and in (c) we report an example of dynamic BW allocation of SCs, with a granularity of 25 Gb/s. Figure 9(a) shows the scenario with 2×100G leaf nodes (each with 4×25 G each, green and blue) that are connected to a 400G (16×25 G, red) hub. This could be the configuration selected in case the hub is connected with 100G transceivers of a 5G antenna.

Next, Fig. 9(b) illustrates the case where four antennas (red) transmit data channels at 50 G (2×25G each), which are simultaneously received by the 400G hub (blue). Note that since the antenna signals are generated dynamically, the total BW can change over time. This application scenario is shown in the example of Fig. 9(c). Here, the evolution of SCs as a function of time and frequency is visualized in a three-dimensional graph. The SCs are sequentially activated/deactivated over time: (i) only 2×SC at $t = 0\,s$; (ii) 5×SC at $t = 100\,s$; (iii) 8×SC at $t = 200\,s$; and (iv) 9×SC at $t = 260\,s$.

III. Intelligent Pluggable Transceiver

The IPT is the key optical device that allows software-configurable optical networks. It supports both P2P and P2MP, providing high capacity and reconfigurability. An example of an IPT is shown in Fig. 10 as a 3D computer rendering in which the TROSA, DSP, ASIC, and integrated capabilities are highlighted.

The TROSA (Fig. 11) is realized through high-density monolithic integration using a minimal number of components, resulting in a highly reliable device that is suitable for mass production. For comparison, other solutions, either in InP or Silicon photonics (SiPh), require more than one optical chip. The InP PIC, shown in detail in Fig. 11, integrates multiple functions (lasers, splitters, amplifiers, and I/Q Mach Zehnder Modulators (MZMs)). As a consequence, the TROSA implementation is

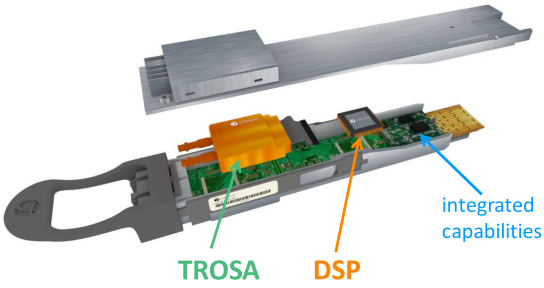

Fig. 10. Computer rendering of a real-time P2MP IPT where we can distinguish the TROSA, DSP, and the integrated capabilities.

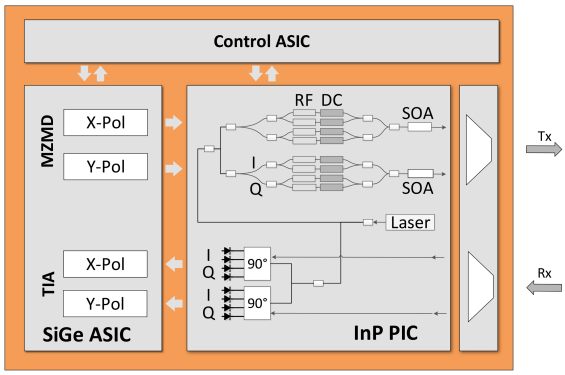

Fig. 11. Schematic of the TROSA with the InP PIC and DSP ASIC.

achieved with a single optical chip, single Thermoelectric Cooler (TEC), single RF ASIC, and single control ASIC, enabling a greatly simplified assembly in a small footprint. Finally, the TROSA is suitable for a variety of DSPs and standard pluggable form factors such as Quad Small Form Factor Pluggable (QSFP), Octal Small Form Factor Pluggable (OSFP), and Centum from-factor pluggable (CFP2).

A. Transmitter-Receiver Optical Sub-Assembly (TROSA)

A high-level schematic of the coherent transceiver is depicted in Fig. 11. It is designed for pluggables comprising an InP PIC with matching RF ASIC implemented in Silicon Germanium (SiGe) and a CMOS control ASIC. The implementation is based on an earlier reported PIC, ASIC, and optical packaging platform, optimized for small form factor pluggable operation [50], [52]. The PIC resides in a single multilayer ceramic gold box, and its temperature is maintained by a TEC for good laser performance. The PIC has a single integrated, widely tunable laser with narrow linewidth and phase-noise to feed both the TX and RX circuits, 4× MZMs, and on-chip amplification to enable output power above 0 dBm with a high Optical Signal-to-Noise-Ratio (OSNR). On the RX side, the output of the tunable laser is split for each polarization and fed into 90° optical hybrids, which are coupled to pairs of balanced photodiodes with BW >35GHz. The use of a single laser enables both the RX and the TX to lock in with the incoming signals. The SiGe ASIC is formed in monolithic Bi-CMOS and includes 4×Mach Zehnder Modulator Driver (MZMD) streams, each with BW >35GHz, and 4×Trans-Impedance Amplifier (TIA) circuits. The control ASIC is a data converter chip that controls the PIC elements directly

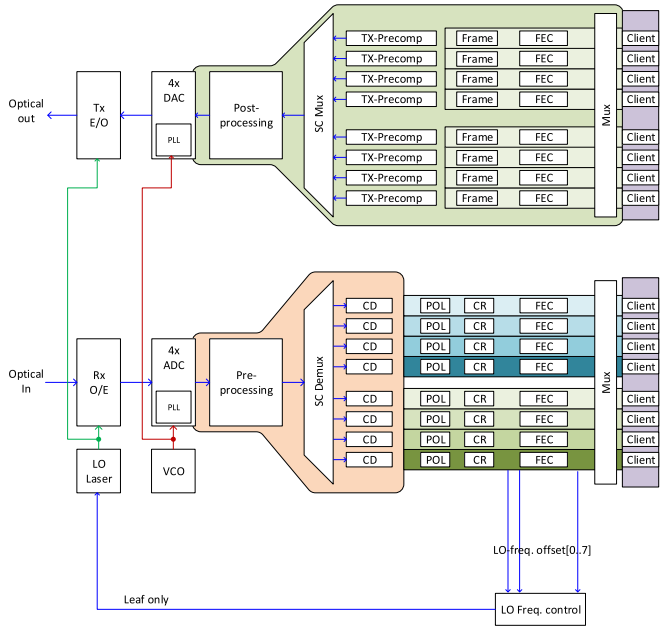

Fig. 12. DSP ASIC block diagram. Upper part: TX DSP; lower part: RX DSP. The diagram is shown for 8×SCs, i.e., a 200G IPT, but may be extended arbitrarily.

and communicates through a Serial Peripheral Interface (SPI) bus with the SiGe chip and the Microcontroller unit (MCU). Lastly, a polarization combiner/splitter block, isolator and a wavelength locker (not shown) are integrated in the TROSA. The chips and the package are designed for minimal power dissipation of typically <7 W, which makes them ideally suited for pluggable form factors.

B. Digital Signal Processing for Digital Subcarrier Multiplexing

Fig. 12 shows the DSP of a transceiver based on DSCM; the upper part is TX DSP, while the lower part is the RX DSP. Data are generated at TX by N clients, and a mux is used to distribute client data to the appropriate SC engines. Next, the FEC encoding and framing is performed, and pilot symbols are added. These are followed by a digital precompensation block, which compensates for component imperfections and applies Nyquist pulse-shaping (∼0.04 roll-off). Finally, individual SCs are digitally multiplexed together with a ∼300 MHz guard band before being outputted through 4×Digital-to-Analog Converters (DAC). The four analog data streams are passed to the TX Electro-Optical (E/O) converter, which prepares the signal for subsequent transmission over the optical fiber.

At the receiver, after Opto-Electrical (O/E) conversion, the data are sampled by 4×Analog-to-Digital Converters (ADC). After signal pre-conditioning (i.e., gain control), the SCs are digitally demuxed into separate processing engines. Each engine has separate chromatic dispersion and matched filtering (CD), and polarization tracking filters (POL), as well as individual clock recovery and Carrier Recovery (CR) circuits; see Fig. 12. A hub node must be able to compensate for different amounts of D_{acc} and polarization effects (e.g., polarization mode dispersion or state-of-polarization changes) from geographically diverse

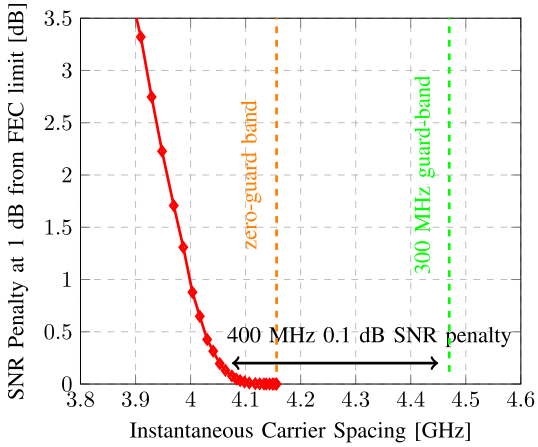

Fig. 13. Signal-to-Noise-Ratio (SNR) penalty in [dB] at 1 dB from FEC limit versus the instantaneous carrier spacing [GHz]. 0 and 300 MHz guard bands are plotted in orange and green.

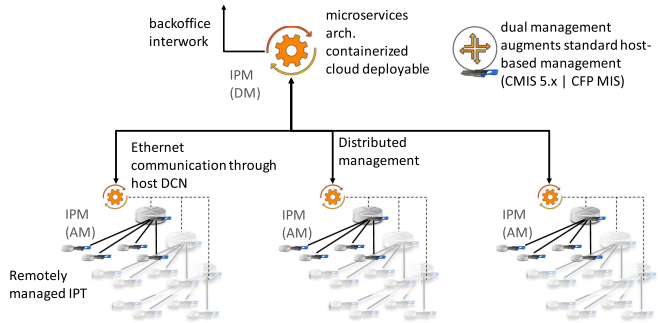

Fig. 14. Network management of densely deployed IPTs, where: C Form-Factor Pluggable (CMIS), Management Interface Specification (MIS), Aggregation Managers (AM), and Domain Manager (DM).

leaf nodes. Similarly, the clock recovery circuit must track the residual timing frequency and phase offsets arising from independent clock sources at the TX and RX. Finally, the FEC decoder corrects errors, and data are transferred from SCs to the appropriate client ports. At the leaf nodes, another control loop locks the frequency of the local oscillator to a known section of the incoming signal from the hub. This loop is DSP-driven and has the ability to track phase and frequency very precisely and provide feedback to adjust leaf lasers at a fast rate. Since the same laser is also used as a transmit laser, the leaf transmit signal tracks changes in the nominal frequency of the hub laser, thus preventing spectral collision from different leaf nodes in the uplink direction. Any further residual frequency variation is removed independently by CR, so that the hub can track small differences from the separate leaf devices. Finally, it is worth pointing out that the utilization of a single laser allows all network applications, including bidirectional transmission on single-fiber, for instance, by selecting/unselecting digital SCs. Fig. 13 shows the SNR penalty for 2×SCs at 4 GBd with 16-QAM, as the instantaneous frequency of one SC is varied. Since the SCs are 4 GBd with a relatively sharp roll-off factor (∼0.04), there is no penalty until the edges of SCs begin to overlap (to the left of the zero guard-band line). The size of the necessary guard-band between SCs depends upon the frequency stability and noise of the lasers that are actively aligned. A large amount of residual frequency noise will mean that SCs from two independent leaf lasers may collide and a larger guard band may be necessary. A 300 MHz guard-band gives a ∼400 MHz tolerance window for residual frequency fluctuations with a SNR penalty of 0.1 dB. A conservative requirement on the maximum laser drift for two lasers, assuming a 4–σ limit, would translate into a standard deviation of ∼50 MHz, which can easily be met by a number of commercial laser devices and frequency locking algorithms.

C. Integrated Capabilities

The DSP has several integrated features that are typically found at the transponder or chassis level. There is intermodule communication, with both an out-of-band channel for discovery and initialization, and in-band GCC channels on each subcarrier. Then, in addition to communication channels, the DSP is also capable of Layer 1 encryption, Link Layer Discovery Protocol (LLDP) for host discovery, packet parsing for traffic routing, and a built-in OSA function. These advanced features facilitate practical benefits such as autodiscovery, power control loops, topology awareness, remote management of leaf optics through the hub optic, and dynamic traffic redistribution via an API interface.

IV. Network Management of Densely Deployed Intelligent Point-to-Multipoint Transceivers

Coherent optical pluggable transceiver configuration is currently carried out based on MSAs that specify both the interface and the available commands in a per-pluggable transceiver form factor. This approach presents a challenge that can stifle innovation due to its inherent characteristics, attachment to specific vendor ecosystems, and dependence on register-based systems. These hinder deployment of advanced features (remote management of far-end pluggables, streaming telemetry, single-fiber designs, threshold crossing alarm settings, and others).

With coherent pluggables evolving towards IPTs, a management approach based on IP/Ethernet communication paths for advanced features plays a key role in accelerating the added value functions of that such pluggable systems are capable of.

Looking at the multiple possible applications of IPTs, a control approach that ensures both compatibility with current register-based configuration, and extended management and configuration capabilities through IP/Ethernet communication paths (the so-called “dual management” approach) becomes highly relevant. This strategy allows for host-agnostic operation while at the same time ensuring an integration path compliant with existing network management architectures.

The way to ensure that IPT innovation cycles become independent of specific host implementations is to deploy a controller that has the capability to provide support for the IP domain level and advanced L_0/L_1 optical transport functions. This management approach avoids relying on router interfaces (designed to interact with L_2/L_3 controllers) for specific L_0/L_1 configuration actions required by coherent optical IPTs and P2MP optical circuits. Fig. 14 illustrates the dual management approach of IPTs with IPM allowing for the improved management of

coherent optical IPTs, augmenting standard host-based configuration capabilities.

Taking into account multiple scenarios and applications of IPTs, the deployment scale is expected to be on the order of thousands of devices, connected to multiple host types. This further benefits from a management approach that is both host agnostic, and upgradeable and extendable, as transceivers evolve at an increasing pace.

IPM is the first implementation of the previously described management architecture that allows for direct IP management of P2MP networks with a distributed and scalable architecture.

IPM allows seamless management and operation of P2P capacity at the L_2/L_3 layer while providing configuration capabilities for the cost and power efficient P2MP traffic aggregation at the L_0/L_1 layer. Intermodule communication — possible via a separate control channel within the same passband spectrum assigned to the data channel — and its inherent capability to manage remote modules, minimizes the number of required IPM-host/module communication channels.

IPM provides access to the rich set of features of IPTs, which includes streaming telemetry, optical spectrum/power analysis, dynamic bandwidth allocation, virtualized network transponder topology discovery functionality, and "transport to L_2/L_3" demarcation points. The demarcation capability is consistent with the split in organizations that have L_2/L_3 and L_0/L_1 subject matter experts.

The capability of managing thousands of devices is inherently enabled by a distributed architecture design that allows the optional deployment of multiple management instances close to the edge of the network (IPM AM) for regional domain management and data aggregation. The core management (IPM DM), through a microservices-based application, provides access to capabilities and exposes management interfaces to optical and IP controllers, allowing for E2E domain and multi-domain network management.

IPM with the dual management paradigm avoids dependencies on the host platform, supporting the evolution of IPTs with an extended set of features made available for network deployment, while providing the current network management architecture that preserves standard host-based management capabilities.

V. Optimized Optics for High-Capacity and High Volume Manufacturability

The achievement of product cost and pricing required for broad market acceptance and stable business operations can be obtained by (i) leveraging the economies of scale that accrue from high-volume manufacturing; (ii) reduction in total parts count by using highly integrated components; and (iii) careful analysis of thermal behavior and signal integrity in the design phase to help ensure a high-yield design compatible with target performance specifications.

Compatibility with high-volume manufacturing processes and equipment must be integrated into the design phase of the product. The consequence of not doing this is a potential redesign of the product during or after the qualification phase. The SotA of CMOS technology makes it economically possible to realize complex electronic systems on a single chip. DSP engines such as the one demonstrated in [4] can be manufactured in large volumes in several silicon foundries. The PIC provides the most convenient way to combine the required photonic components and achieve the desired functionality [53]. Two technologies, SiPh and InP are available for the implementation of PICs. Of these, InP is the only one that supports the integration of passive components, such as waveguides and splitters, with active photonic devices, such as tunable lasers, IQ Mach-Zehnder Modulator (IQ-MZM), and PIN detectors [50], [54], [55]. The ability to monolithically integrate lasers reduces the number of critical signal interfaces, simplifies packaging, and reduces the physical volume of the end product. Complex optoelectronic functions, manufactured with InP PIC technology [52] have been used in fielded optical communication systems for more than 20 years, attesting to the stability and reliability of this technology. Implementing a specific design is accomplished using pick-and-place and active alignment tools, both of which are capable of high-volume throughput.

VI. Redefining access/metro Networks – a Techno-Economic Perspective

Section II-C5 reported on the various types of applications that an IPT with P2MP capabilities can enable. In this context, several studies have been carried out to assess the economic benefits of this solution. This section is divided into two parts: the first provides a recap of previous published works, while the second extends the work presented in [56], by showing that the use of P2MP transceivers can further improve the network efficiency.

A. Prior Techno-Economic Analyses on Point-to-Multipoint Optical Networks

Several studies have been published showing the economic benefits of P2MP IPT. In [57], the authors reported how in access/metro networks, the deployment of P2MP transceivers can lead to savings if the cost of an IPT is below 1.5× the cost of an equivalent module deployed in a P2P case. As explained in [57], the advantage is a direct consequence of the P2MP capabilities of IPTs. Next, in [33], we evaluated 226 horseshoe topologies in the national network of British Telecom (BT) [33]. Here, we assumed a constant traffic growth of 30% over 5 years and compared a filterless approach with traditional coherent transceivers, with the proposed coherent P2MP approach. Subsequently, we performed transmission analyses to verify that all links could be closed with a sufficient OSNR margin, and compared the techno-economics of the solutions. The results are reported in Fig. 15, and show that a CAPEX savings up to 75% [33] can be achieved by designing the network with P2MP transceivers instead of P2P.

A similar analysis was carried out with two realistic topologies provided by Telecom Italia Mobile (TIM) [42]. As with our previous analyses of the BT network, we considered horseshoe topologies and a filterless architecture. The main results are reported in Fig. 16. The investigation focused on real traffic

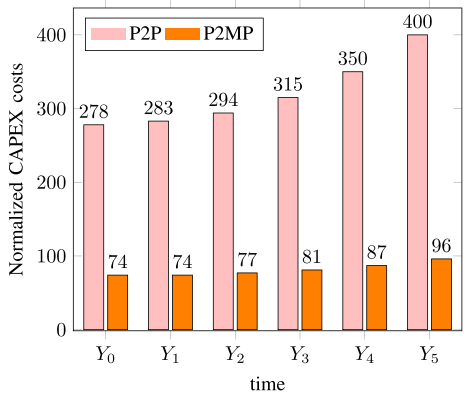

Fig. 15. Normalized Capital Expenditure (CAPEX) saving comparison between the case with P2P and P2MP pluggables [33].

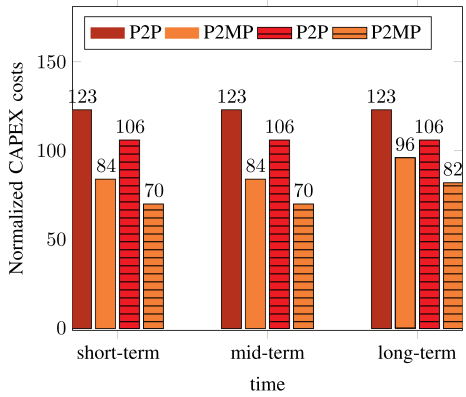

Fig. 16. Savings in terms of normalized CAPEX between the case with P2P and P2MP pluggables: without horizontal pattern, urban/industrial topology; with, suburban/rural one.

matrices as discussed in [42], and CAPEX has been evaluated from short- to medium- to long-term traffic growth, according to the operator's forecast [42]. The optical layer analysis focused on different configurations, with the aim of maximizing the number of horseshoes that could be optically aggregated. Without modifying the optical infrastructure, and providing OSNR margins >6 dB, we achieved the results presented in Fig. 16, where we observe CAPEX savings of 32%. It was also shown that CAPEX savings could be increased to 41% in the short-term scenario for the same topology by further traffic aggregation (i.e., combining more links into a single optical domain) through additional investment in the OLS.

Finally, in collaboration with Telefónica, we performed a third study [29], where we aimed at maximizing the number of HL $_5$ nodes that can be connected to a given network.[3] The analysis first evaluated the optical performance and the number of HL_4 nodes that could be crossed with a sufficient OSNR margin. This revealed, for example, that 8× HL_5 nodes could be connected while traversing 4×HL_4 routers, before reaching HL_3. This translated into the CAPEX savings reported in Fig. 17, where we show the case for 8× HL_5, with different traffic loads for the

[3]In Telefónica denomination, HL stands for hierarchic layer, and HL_5 is the access/metro aggregation, while the remaining $HL_4 \rightarrow HL_1$ represent the entire network from metro to core.

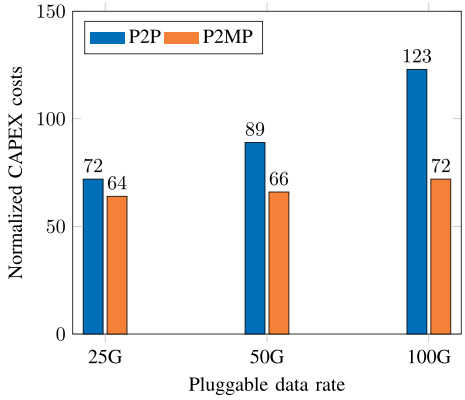

Fig. 17. Statistical analysis assessing the normalized CAPEX costs of routing by-pass with P2P and with P2MP pluggables assuming 8 HL_5 nodes.

nodes. P2MP clearly requires a lower number of transceivers for aggregation and also a lower occupation of the router ports. The savings increase as the traffic load increases, with values around 42% [29], regardless of the number of HL_5 elements connected to the network.

In conclusion, P2MP provides an intrinsic increased flexibility in managing and using the capacity within the given spectrum. This allows users to match hardware utilization with real needs, e.g., traffic, cost, bandwidth demand. Different architectures and applications will drive different solutions. In some instances, changes are not needed in the routing layer architecture to realize savings, as we simplify the aggregation methodology within a single routing layer. In others, users may consolidate and combine routing layer functions.

B. Techno-Economic Analysis With Intelligent Pluggable Transceivers in RON.

A techno-economic analysis was performed on a horseshoe network (also known as an open ring) with a symmetrical traffic profile in which the same amount of capacity of each leaf node is connected to both hubs, as illustrated in Fig. 18(a). We modeled three scenarios with 4, 6, and 9 leaf nodes per horseshoe network with dual hubs and redundant hardware at each leaf site for protection. The initial traffic from each leaf to each hub is 100G, and we assume a traffic growth of 100G per year for each leaf. This study is based on the network profile described in [56].

For each scenario (4, 6 and 9 leaf nodes), we compared three coherent-based solutions: 400ZR w/Regen (Fig. 18(b)) [12], 400ZR+ w/Express Fig. 18(c) [58], and 400 G XR Fig. 18(d) [43]. In 400ZR w/Regen, traffic between the source and destination is regenerated at intermediate leaf sites using 400G ZR pluggables. In the 400ZR+ w/Express solution, traffic is optically expressed at intermediate leaf sites leveraging the greater optical performance of 400ZR+. From a line system perspective, this can be implemented in several different ways, including the use of fixed or reconfigurable optical add/drop multiplexers or a filterless line system with passive couplers and combiners. Both 400ZR w/Regen and 400ZR+ w/Express operate in a P2P configuration along the horseshoe ring. However, a single 400G ZR pluggable can "regen" multiple 100G streams, and it is assumed that a dual router (4 Terabit (4T) for

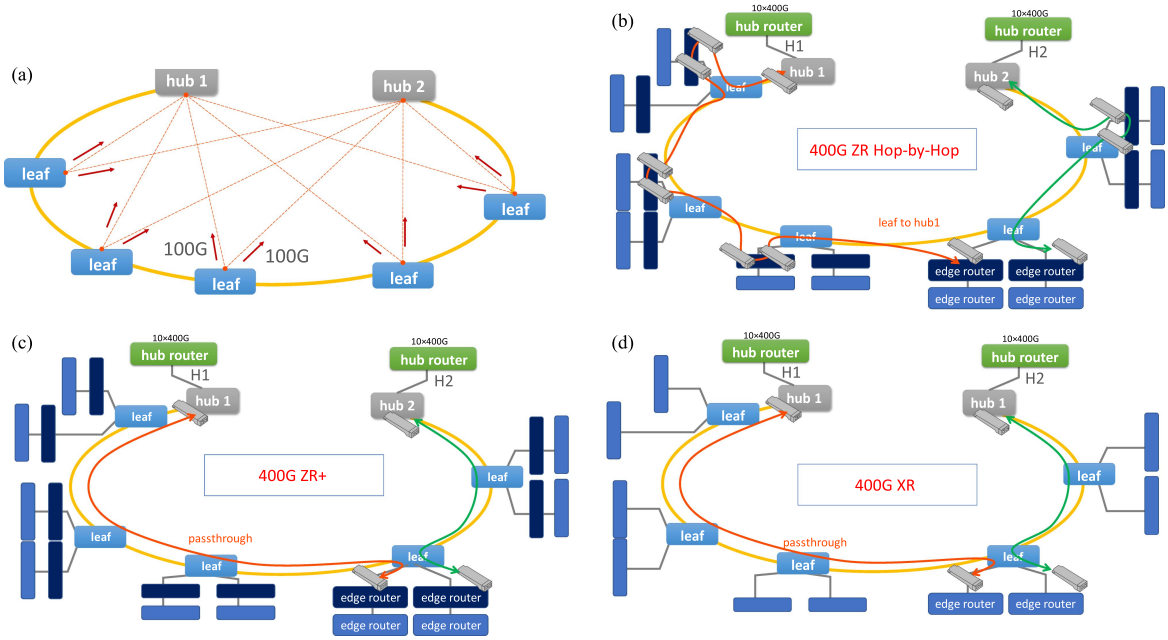

Fig. 18. Considered scenario for the Routed Optical Networks (RON) analysis: (a) general horseshoe topology; (b) Horseshoe with 400ZR Hop-by-Hop P2P (400ZR w/Regen); (c) Horseshoe with 400ZR+ P2P (400ZR+ w/Express); (d) Horseshoe with 400G P2MP (400 G XR).

400G and a 1T router for lower speeds, interconnected with grey optics) deployment will provide a lower granularity of service. In our proposed solution (400 G XR), a H&S traffic profile is assumed, where a 400G XR is deployed at each hub site and 100G or 400G XR at remote leaf nodes. Given the granularity of 25Gb/s, a single 1T router is assumed at each leaf node. Our transport layer analysis covers three aspects: (i) the number of coherent pluggables (400ZR w/Regen, 400ZR+ w/Express, 400 G XR); (ii) normalized CAPEX costs for transceivers and router ports; and (iii) port efficiency calculated by the volume of traffic transmitted over each coherent pluggable port versus the total capacity of said port. There are also secondary effects not covered here. The 400ZR w/Regen architecture can use fewer optical amplifiers, and the costs of the router layers will be different between the three architectures. This will be part of future work.

The results of our analysis are reported in Table II and reveal that the solutions 400ZR+ w/Express and 400 G XR require a significantly lower number of coherent pluggables compared to 400ZR w/Regen (see Table II, row 1). This can be explained by the fact that traffic carried over 400ZR+ w/Express and 400 G XR is not required to be "regenerated" at intermediate sites. The number of 400G ZR coherent pluggables increases significantly as we increase traffic and the number of leaf nodes from 4 to 9. When comparing 400G XR to 400G ZR+ P2P, we observe that the number of coherent pluggables for 400G XR is lower as traffic increases over the 5-year period. This is due to the fact that 400 G XR operates in a P2MP network and, therefore, requires fewer coherent pluggables at the hub sites. In terms of CAPEX[4], 400 G XR provides the lowest figure in all three scenarios (4, 6 and 9 leaf nodes) and over modeled traffic growth (an additional 100G per year per leaf), Table II, row 2. This can be explained by the fact that 400 G XR has fine granularity and therefore only a smaller and more efficient router is used at the leaf sites versus two interconnected routers (4T and 1T) to provide this granularity. Furthermore, a single coherent pluggable 400 G XR can be simultaneously connected to up to 16 leaf nodes (even though we only modeled up to 9 leaf nodes), thus reducing the number of coherent pluggables at the hub sites. We also realized that CAPEX increases significantly for 400ZR w/Regen solutions with increasing traffic and as we increase the number of leaf nodes. This can be explained by the fact that each additional leaf site will be required to "regen" the traffic, thus driving the need for more routers and 400G ZR pluggables.

The port efficiency was also modeled and the results are reported in Table II, row 3. The solution based on 400 G XR has the highest port efficiency by far. This can be explained by the fact that the 400 G XR pluggables at the leaf sites exactly match the modeled growth rate (100G/leaf/year), so there is no wasted port capacity. This has become clear as traffic grows compared to 400ZR w/Regen and 400ZR+ w/Express solutions, where only a fraction of the total port capacity is used (e.g., 100G of a 400G port, equivalent to 25% efficiency). Given the need to "regen" traffic at each intermediate node, the 400ZR w/Regen solution has the lowest port efficiency.

The main assumptions employed in this analysis are:

- 400ZR+ w/Express has the same price as 400 G XR
- 400ZR w/Regen is 42% the price of 400ZR+ w/Express and 400 G XR
- 100G XR is 42% the price of 400ZR+ w/Express and 400 G XR
- The price of a 4T router (10×400G ports) at hub sites is the same as a 4T router (mix of 400G line and 100G client ports) at leaf sites
- The price of a 1T router is 33% of a 4T router.

[4]It should be noted that the CAPEX has been normalized for each leaf node scenario, with respect to the highest cost.

TABLE II
TECHNO-ECONOMIC ANALYSIS COMPARING THE THREE SCENARIOS IN FIG. 18 IN TERMS OF THE NUMBER OF COHERENT PLUGGABLES (ROW 1); NORMALIZED CAPEX (ROW 2) AND PORT EFFICIENCY (ROW 3)

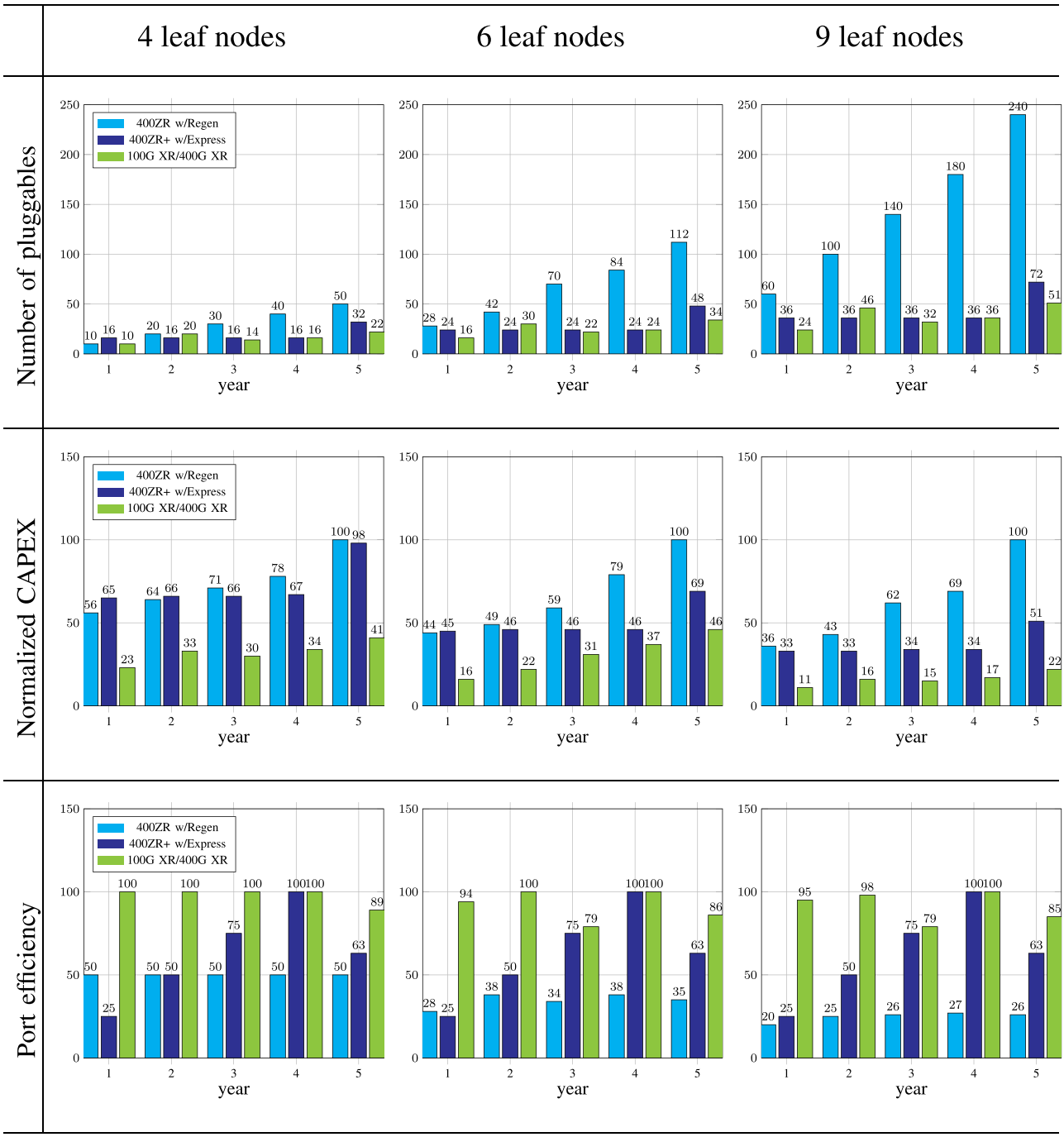

VII. EXPERIMENTAL VERIFICATION OF POINT-TO-MULTIPOINT TRANSCEIVERS

This section is divided into two parts: the description of the experimental setup, which has been constructed around real-time P2MP transceivers realized on EVBs, with the aim of preparing for the production of 100G/200G/400G transceivers, and the first-ever measurements of real-time coherent P2MP transceivers, where we show the detection of various types of low-speed leaf nodes (100G/200G) by a high-speed one (400G, hub) and vice-versa in B2B configuration.

A. Back-to-Back Setup

Fig. 19 illustrates the experimental setup with the configurations for uplink (a) and downlink (b) directions. These experiments were carried out using prototypes mounted on EVBs, with DSP and optics supporting the realization of IPTs. Prior

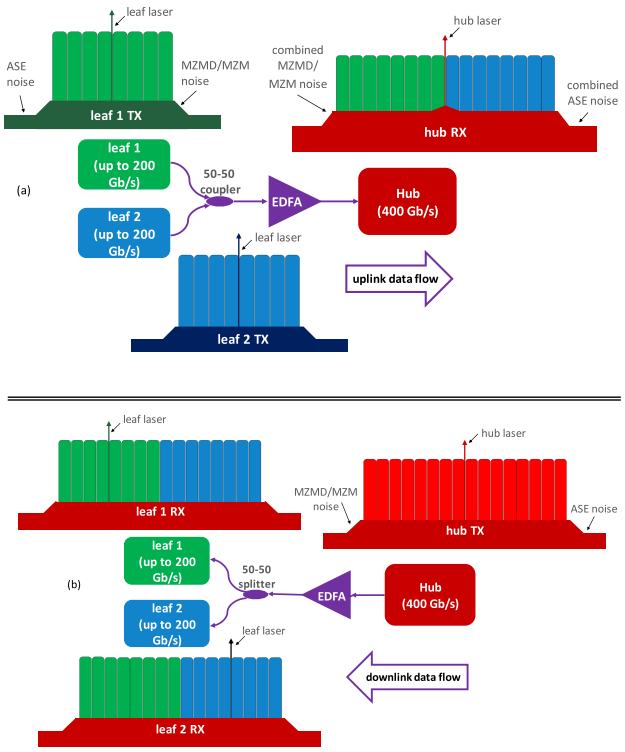

Fig. 19. Experimental setup for real-time validation of P2MP transceivers. At the two leaf nodes we transmit either at 100G (4×25G) or 200G (8×25G). In both configurations, the leaf nodes are connected to a hub operating at 400G (16×25G). (a) Uplink direction, (b) Downlink direction. All channels/SCs employ dual-polarization with 16-QAM at 4 GBd.

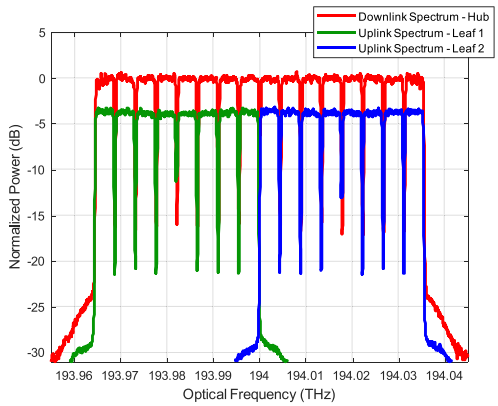

Fig. 20. Transmitted spectra of two leaf nodes at 2×200G (green and blue) and from the 400G hub (red).

to the experiments, calibrations were performed on each prototype to compensate for front-end Linear Time Invariant (LTI) impairments. The prototypes of this setup are fully controlled by product Firmware (FW) and all measurement data are reported in real-time DSP.

In both uplink and downlink scenarios, we consider two prototype leaf nodes[5] at 100G/200G, connected in a B2B configuration to a 400G hub node, on the left-hand side in green and blue, and on the right-hand side in red. In the uplink direction (Fig. 19(a)), the two leaf nodes are optically aggregated by a 50–50% passive optical combiner to form a 400G aggregated optical channel with 16×SCs, which is received by the 400G P2MP hub. The power level of each leaf is adjusted to achieve the same level before being received at the hub. In the downlink direction, the signal from the 400G hub is split 50–50% passively to the two leaf nodes, as shown in Fig. 19(b), and each leaf receives all SCs from the hub. The DSP must select and process its assigned SCs while ignoring the rest of the SCs.

To prevent spectral collision between SCs from the two leaf nodes, each leaf laser must be wavelocked based on DSP feedback to the hub broadcast spectrum, although each at a different offset. As depicted in Fig. 19(a), the laser for leaf 1 is located in the middle of the lower sideband SCs and the laser for leaf 2 is located in the middle of the upper sideband SCs. The hub laser transmits at 194 THz.

As shown by the inset spectra in Fig. 19, the two leaf nodes are configured for 200G (8SCs) operation, utilizing dual polarization 16-QAM with ∼4 GBd per SC, each carrying 25Gb/s. Consequently, the hub has been configured for 400G with 16 SCs operating at the same per-SC symbol rate and modulation format.

By simply reconfiguring the SC assignment of each leaf, it is possible to change the speed of the uplink. Here, we also report on a P2MP link with 2×100G, i.e., 4SCs per leaf node using the same setup.

It should be mentioned that in our experiments, the noise sources consist of MZMD and MZM noise and nonlinearity, plus Amplified Spontaneous Emission (ASE) from integrated SOAs and the line Erbium Doped Fiber Amplifiers (EDFAs).

B. *Spectra and Constellation Results*

Based on the experimental setup of Fig. 19, we show two important use cases of P2MP transmission.

a) Multipoint-to-point scenario: 2×200G (leaf) → 400G (hub): First, we evaluated the performance of 2×200G leaf nodes connected to a single 400G hub node. Fig. 20 shows the PSD of transmitted spectra for downlink and uplink. Fig. 21 reports the PSD observed at the hub DSP, as directly reported by the FW. Here, we also report the 16 SCs — eight from each leaf node — and the constellation diagrams corresponding to the polarization-multiplexed signal for each SC. As the spectrum is measured at the beginning of the DSP chain, the response of the analog front-end is still visible as a power variation throughout the 16 SCs. This power imbalance between SCs is removed digitally using gain control circuits after demuxing. In addition, the positions of the two leaf lasers are visible in this PSD: leaf 1 between SCs 4 and 5, and leaf 2 between SCs 12 and 13.

The wide-enough gaps (∼300 MHz) between each SC ensure that there is no collision between SCs coming from different leaf nodes, as also shown in Fig. 13. Observing the dual-polarization constellations, we can see the recovered 16-QAM data in each SC, indicating that the DSP is capable not only of processing the local oscillator offset, but also of correctly performing clock recovery, although not all data come from the same TX. As expected, in this experiment we achieve error-free P2MP

[5]It should be noted that in the insets of Fig. 19, we drew only the case with 200G leaf nodes.

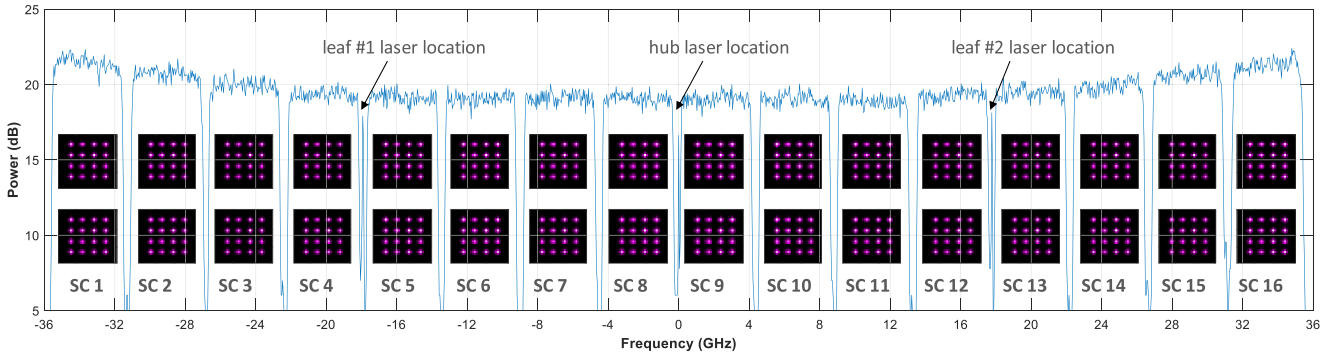

Fig. 21. Detection of 2×200G leaf uplink spectrum by the hub RX, which operates at 400G. All 16 dual-polarization constellations (X- and Y-polarizations plotted separately) are transmitting data; and the received spectra from the two leaf nodes as seen by hub Rx. Transmission was error-free after the FEC for all present SCs.

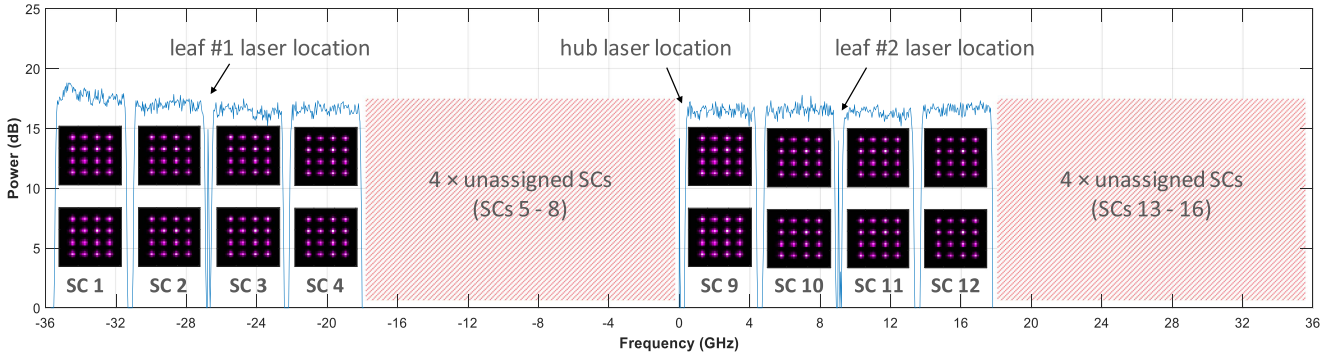

Fig. 22. Detection of 2×100G leaf uplink spectrum by the hub RX, which operates at 400G: Eight of the 16 dual-polarization constellations (X- and Y-polarizations plotted separately), where only the one 1–4 and 9–12 are transmitting data; and the received spectra from the two leaf nodes as seen by hub Rx. Transmission was error-free after the FEC for all present SCs.

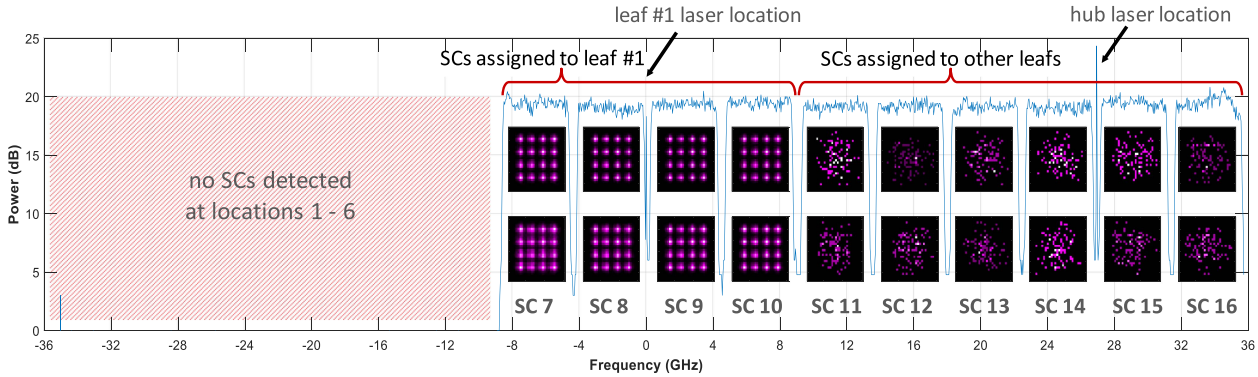

Fig. 23. Detection of the 400G hub downlink spectrum by leaf 1, which operates at 100G: The 16 dual-polarization constellations, where only the center four SCs carry data intended for this leaf; and the received spectra from the hub node as seen by the leaf 1 Rx. The leaf laser is offset from the hub laser by six SCs, resulting in no optical power at the six left-most SC positions of the PSD. The center four SCs (7–9) are assigned to leaf 1, and are recovered error-free after FEC, while the SCs 11–16 are assigned to other leaf nodes, and are not processed.

operation, and the hub DSP's FEC engine reports no post-FEC failures in the transmitted data payloads.

b) Point-to-multipoint scenario: 400G → 4×100G: In the second demonstration, we emulate a P2MP scenario where a 400G hub is communicating with 4×100G leaf nodes, with only two of the four nodes currently active. In this scenario, the 16 SCs from the hub are split into four groups of four SCs, with each group supporting communication with a 100G leaf. We assign leaf 1 to the leftmost group (SCs 1–4) and leaf 2 to the center right group (SCs 9–12), leaving the remaining eight SCs unassigned. This results in the optical spectra transmitted in Fig. 9(a). The PSD seen by the hub DSP (uplink direction) is reported in Fig. 22. Here, we see the two groups of 4×SCs — 1 group for each of the current leaf nodes — and some empty spectrum, where two additional 100G leaf nodes could be added in the future.

We then show the constellation diagrams received in the inset in each SC and confirm that the data from each leaf node are post-FEC error-free. Furthermore, we also plot the PSD seen by DSP in leaf 1 (downlink direction) in Fig. 23. The hub still transmits 16 SCs, but since this leaf was assigned the leftmost group of four SCs on the hub, its laser is offset from the hub laser by six SC, as shown in Fig. 9(a). The result is the asymmetric PSD seen in Fig. 23; there is no optical signal in the positions for SCs 1–6 due to the six-SC offset between hub and leaf lasers, the four SCs carrying data assigned to leaf 1 are in positions 7–10, and the data from the hub on SCs 11–16 are intended for other leaf nodes. The RX DSP in the leaf processes the four central SCs and the data are recovered correctly (see constellation diagrams in Fig. 23), while ignoring the remaining six SCs (the rightmost ones in the figure) within the bandwidth of the receiver.

VIII. The Importance of Standardization and a Healthy Supply Chain Ecosystem

The DSCM-based P2MP solution described here supports scalable traffic requirements, high capacity, and extreme flexibility and multigenerational deployment. This enables a paradigm shift as discussed in Section II. Such a paradigm shift will require a joint effort of operators, system vendors, and component suppliers to standardize both software and hardware, realizing an open and disaggregated ecosystem. To this end, an MSA [43] has been formed to foster collaboration that will advance the development of DSCM-based technology and services, accelerate the adoption of intelligent coherent P2P and P2MP network architectures, and drive standardization of networking interfaces to ensure ease of multi-vendor interoperability and an open, multi-source solution ecosystem [43]. The MSA will publish a series of specifications that allow disaggregation of the network and IPT management, design of IPT modules, and design of components within IPT modules, including the TROSA and DSP ASIC. IPT module interfaces are based on existing hardware standards from other MSAs such as those for QSFP-DD [59], CFP2 [60], and OSFP [61]. The TROSA specification will be based on existing specifications, such as those published by the OIF [62] with any required deviations clearly identified.

Standardization of DSCM technology will ensure a flexible ecosystem of components and a robust supply chain, meeting demands of service providers to minimize supply risk and promote competition among suppliers. With standardization, the benefits of DSCM technology across multiple applications, including P2P long-haul, metro transport, PON overlay, and 5G front-haul justify investments in technology and will ensure that economies of scale are realized.

IX. Summary

This section summarizes the highlights of this manuscript, reporting the motivations, challenges, and potentialities of software-configurable optical networks enabled by digital subcarrier multiplexing (DSCM).

Throughout this article, we presented the key enablers of the technology we are proposing, starting with DSCM, which is the primary building block to realize point-to-point (P2P) and point-to-multipoint (P2MP) transceivers.

Next, we explained the main features of intelligent pluggable transceivers (IPT) and how to manage and control them in a scenario of densely deployed networks. We also presented a comprehensive techno-economic analysis for the most common type of network topologies, showing the benefits in terms of required pluggables, reduced Capital Expenditure (CAPEX), and port efficiency, all with respect to the current state-of-the-art (SotA). In Section VII, we reported the first-ever experimental real-time validation of coherent transceivers with P2P and P2MP capabilities.

The technology proposed in this work has the potential to revolutionize optical networks. It enables high-capacity P2P and P2MP links for access and metro networks. As assessed by various studies, it also leads to significant cost savings in CAPEX/OPEX, as well energy reduction and less need for human intervention. This last feature is clearly one of the most important advantages obtained through the realization of software-configurable networks.

References

[1] "Cisco Annual Internet Report (2018–2023) White Paper," 2020. [Online]. Available:https://www.cisco.com/c/en/us/solutions/collateral/executive-perspectives/annual-internet-report/white-paper-c11-741490.html

[2] T. Mizuochi et al., "A comparative study of DPSK and OOK WDM transmission over transoceanic distances and their performance degradations due to nonlinear phase noise," *J. Lightw. Technol.*, vol. 21, no. 9, pp. 1933–1943, Sep. 2003.

[3] B. Wedding, B. Franz, and B. Junginger, "10-Gb/s optical transmission up to 253 km via standard single-mode fiber using the method of dispersion-supported transmission," *J. Lightw. Technol.*, vol. 12, no. 10, pp. 1720–1727, Oct. 1994.

[4] H. Sun et al., "800G DSP ASIC design using probabilistic shaping and digital sub-carrier multiplexing," *J. Lightw. Technol.*, vol. 38, no. 17, pp. 4744–4756, Sep. 1, 2020, doi: 10.1109/JLT.2020.2996188.

[5] S.-C. Wang et al., "Coherent DSP and system integration technologies for 800G," in *Proc. Opt. Fiber Commun. Conf.*, 2022, pp. 1–3.

[6] M. Seimetz, *High-Order Modulation for Optical Fiber Transmission,* vol. 143. Berlin, Germany: Springer, 2009.

[7] D. Welch et al., "Point-to-multipoint optical networks using coherent digital subcarriers," *J. Lightw. Technol.*, vol. 39, no. 16, pp. 5232–5247, Aug. 15, 2021, doi: 10.1109/JLT.2021.3097163.

[8] A. Ferrari et al., "Assessment on the achievable throughput of multi-band ITU-T G. 652.D fiber transmission systems," *J. Lightw. Technol.*, vol. 38, no. 16, pp. 4279–4291, Aug. 2020.

[9] J. Renaudier et al., "107 Tb/s transmission of 103-nm bandwidth over 3× 100 km SSMF using ultra-wideband hybrid Raman/SOA repeaters," in *Proc. Opt. Fiber Commun. Conf. Exhib.*, 2019, pp. 1–3.

[10] B. J. Puttnam, G. Rademacher, and R. S. Luís, "Space-division multiplexing for optical fiber communications," *Optica*, vol. 8, no. 9, pp. 1186–1203, 2021.

[11] A. Nespola et al., "Transmission of 61 C-band channels over record distance of hollow-core-fiber with l-band interferers," *J. Lightw. Technol.*, vol. 39, no. 3, pp. 813–820, Feb. 1, 2021, doi: 10.1109/JLT.2020.3047670.

[12] "Implementation agreement 400ZR," Mar. 10, 2020. [Online]. Available: https://www.oiforum.com/wp-content/uploads/OIF-400ZR-01.0_reduced2.pdf

[13] P. Wright, R. Davey, and A. Lord, "Cost model comparison of ZR/ZR modules against traditional WDM transponders for 400G IP/WDM core networks," in *Proc. Eur. Conf. Opt. Commun.*, 2020, pp. 1–4.

[14] P. Pavon-Marino, N. Skorin-Kapov, M. Bueno-Delgado, J. Bäck, and A. Napoli, "On the benefits of point-to-multipoint coherent optics for multilayer capacity planning in ring networks with varying traffic profiles," *J. Opt. Commun. Netw.*, vol. 14, no. 5, pp. B30–B44, 2022.

[15] O. Ayoub, A. Bovio, F. Musumeci, and M. Tornatore, "Survivable virtual network mapping with fiber tree establishment in filterless optical networks," *IEEE Trans. Netw. Service Manag.*, vol. 19, no. 1, pp. 37–48, Mar. 2022.

[16] D. Gomez-Barquero, D. Navrátil, S. Appleby, and M. Stagg, "Point-to-multipoint communication enablers for the fifth generation of wireless systems," *IEEE Commun. Standards Mag.*, vol. 2, no. 1, pp. 53–59, Mar. 2018.

[17] J. S. Wey, "The outlook for PON standardization: A tutorial," *J. Lightw. Technol.*, vol. 38, no. 1, pp. 31–42, Jan. 1, 2020, doi: 10.1109/JLT.2019.2950889.

[18] D. Che, P. Iannone, G. Raybon, and Y. Matsui, "200 Gb/s Bi-directional TDM-PON with 29-dB power budget," in *Proc. Eur. Conf. Opt. Commun.*, 2021, pp. 1–3.

[19] M. Xu, Z. Jia, H. Zhang, L. A. Campos, and C. Knittle, "Intelligent burst receiving control in 100G coherent PON with 4×25G TFDM upstream transmission," in *Proc. Opt. Fiber Commun. Conf.*, Optica Publishing Group, 2022, pp. 1–3.

[20] N. Sambo et al., "Next generation sliceable bandwidth variable transponders," *IEEE Commun. Mag.*, vol. 53, no. 2, pp. 163–171, Feb. 2015.

[21] W. Shieh, X. Yi, Y. Ma, and Q. Yang, "Coherent optical OFDM: Has its time come?," *J. Opt. Netw.*, vol. 7, no. 3, pp. 234–255, 2008.

[22] T. A. Eriksson, F. Buchali, W. Idler, L. Schmalen, and G. Charlet, "Electronically subcarrier multiplexed PM-32QAM with optimized FEC overheads," in *Proc. Opt. Fiber Commun. Conf. Exhib.*, 2017, pp. 1–3.

[23] F. P. Guiomar, L. Bertignono, A. Nespola, and A. Carena, "Mitigation of transceiver bandwidth limitations using multi-subcarrier signals," in *Proc. IEEE 19th Int. Conf. Transparent Opt. Netw.*, 2017, pp. 1–4.

[24] F. Buchali et al., "Study of electrical subband multiplexing at 54 GHz modulation bandwidth for 16QAM and probabilistically shaped 64QAM," in *Proc. 42nd Eur. Conf. Opt. Commun.*, 2016, pp. 1–3.

[25] Y. Zhang, M. O'Sullivan, and R. Hui, "Digital subcarrier multiplexing for flexible spectral allocation in optical transport network," *Opt. Exp.*, vol. 19, no. 22, pp. 21880–21889, 2011.

[26] M. Qiu et al., "Digital subcarrier multiplexing for fiber nonlinearity mitigation in coherent optical communication systems," *Opt. Exp.*, vol. 22, no. 15, pp. 18770–18777, 2014.

[27] L. B. Du and A. J. Lowery, "Optimizing the subcarrier granularity of coherent optical communications systems," *Opt. Exp.*, vol. 19, no. 9, pp. 8079–8084, 2011.

[28] J. Bäck et al., "Hubbedness: A metric to describe traffic flows in optical networks and an analysis of its impact on efficiency of point-to-multipoint coherent transceiver architectures," in *Proc. Eur. Conf. Opt. Commun.*, 2021, pp. 1–4.

[29] A. Napoli et al., "Enabling router bypass and saving cost using point-to-multipoint transceivers for traffic aggregation," in *Proc. Opt. Fiber Commun. Conf.*, 2022, pp. 1–3.

[30] L. Velasco et al., "Autonomous and energy efficient lightpath operation based on digital subcarrier multiplexing," *IEEE J. Sel. Areas Commun.*, vol. 39, no. 9, pp. 2864–2877, Sep. 2021.

[31] T. Rahman et al., "Digital subcarrier multiplexed hybrid QAM for data-rate flexibility and roadm filtering tolerance," in *Proc. Opt. Fiber Commun. Conf.*, 2016, pp. 1–3.

[32] D. Welch et al., "Digital subcarriers: A universal technology for next generation optical networks," in *Proc. Opt. Fiber Commun. Conf.*, Optica Publishing Group, 2022, pp. 1–3.

[33] J. Bäck et al., "CAPEX savings enabled by point-to-multipoint coherent pluggable optics using digital subcarrier multiplexing in metro aggregation networks," in *Proc. Eur. Conf. Opt. Commun.*, 2020, pp. 1–4.

[34] A. Napoli et al., "Live network demonstration of point-to-multipoint coherent transmission for 5G mobile transport over existing fiber plant," in *Proc. Eur. Conf. Opt. Commun.*, 2021, pp. 1–4.

[35] T. Pfeiffer, P. Dom, S. Bidkar, F. Fredricx, K. Christodoulopoulos, and R. Bonk, "PON going beyond FTTH [invited tutorial]," *J. Opt. Commun. Netw.*, vol. 14, no. 1, pp. A31–A40, 2022.

[36] D. Zhang, D. Liu, X. Wu, and D. Nesset, "Progress of ITU-T higher speed passive optical network (50G-PON) standardization," *J. Opt. Commun. Netw.*, vol. 12, no. 10, pp. D99–D108, 2020.

[37] A. Arnould et al., "Field trial demonstration over live traffic network of 400 Gb/s ultra-long haul and 600 Gb/s regional transmission," in *Proc. Eur. Conf. Opt. Commun.*, 2020, pp. 1–4.

[38] "G.984.1: Gigabit-Capable Passive Optical Networks (GPON): General Characteristics," Link to the document.

[39] P. Poggiolini, Y. Jiang, A. Carena, G. Bosco, and F. Forghieri et al., "Analytical results on system maximum reach increase through symbol rate optimization," in *Proc. Opt. Fiber Commun. Conf.*, OSA Technical Digest (online) (Optica Publishing Group, 2015), 2022, pp. 1–3.

[40] R. Borkowski et al., "FLCS-PON–A 100 Gbit/s flexible passive optical network: Concepts and field trial," *J. Lightw. Technol.*, vol. 39, no. 16, pp. 5314–5324, Aug. 2021.

[41] J. Zhang and Z. Jia, "Coherent passive optical networks for 100G/λ-and-beyond fiber access: Recent progress and outlook," *IEEE Netw.*, vol. 36, no. 2, pp. 116–123, Mar./Apr. 2022.

[42] J. Bäck et al., "A filterless design with point-to-multipoint transceivers for cost-effective and challenging metro/regional aggregation topologies," in *Proc. IEEE Int. Conf. Opt. Netw. Des. Model.*, 2022, pp. 1–6.

[43] "open XR forum," Checked on Sep. 29, 2022. [Online]. Available: https://www.openxrforum.org/

[44] P. J. Winzer, "Chapter 8 - Transmission system capacity scaling through space-division multiplexing: a techno-economic perspective," in *Optical Fiber Telecommunications VII*. A. E. Willner, Ed., Academic Press, 2020, pp. 337–369.

[45] R. Olshansky, V. A. Lanzisera, and P. M. Hill, "Subcarrier multiplexed lightwave systems for broad-band distribution," *J. Lightw. Technol.*, vol. 7, no. 9, pp. 1329–1342, Sep. 1989.

[46] R. Hui, B. Zhu, R. Huang, C. T. Allen, K. R. Demarest, and D. Richards, "Subcarrier multiplexing for high-speed optical transmission," *J. Lightw. Technol.*, vol. 20, no. 3, pp. 417–427, Mar. 2002, doi: 10.1109/50.988990.

[47] M. Stephens et al., "Trans-atlantic real-time field trial using super-Gaussian constellation-shaping to enable 30 Tb/s capacity," in *Proc. Opt. Fiber Commun. Conf. Exhib.*, 2021, pp. 1–3.

[48] A. R. Brusin, F. Guiomar, A. Lorences-Riesgo, P. Monteiro, and A. Carena, "Enhanced resilience towards ROADM-induced optical filtering using subcarrier multiplexing and optimized bit and power loading," *Opt. Exp.*, vol. 27, no. 21, pp. 30710–30725, 2019.

[49] P. Poggiolini, Y. Jiang, A. Carena, G. Bosco, and F. Forghieri, "50Gb/s real-time transmissions with upstream burst-mode for 50G-PON using a common soa pre-amplifier/booster at the olt," in *Proc. Opt. Fiber Commun. Conf. Exhib.*, 2015, pp. 1–3.

[50] S. Porto et al., "Demonstration of a 2× 800 Gb/s/wave coherent optical engine based on an InP monolithic PIC," *J. Lightw. Technol.*, vol. 40, no. 3, pp. 664–671, Feb. 1, 2022, doi: 10.1109/JLT.2021.3121284.

[51] R. Bonk et al., "50G-PON: The first ITU-T higher-speed PON system," *IEEE Commun. Mag.*, vol. 60, no. 3, pp. 48–54, Mar. 2022.

[52] G. E. Hoefler et al., "Foundry development of system-on-chip InP-based photonic integrated circuits," *IEEE J. Sel. Topics Quantum Electron.*, vol. 25, no. 5, pp. 1–17, Oct. 2019.

[53] F. Kish et al., "System-on-chip photonic integrated circuits," *IEEE J. Sel. Topics Quantum Electron.*, vol. 24, no. 1, pp. 1–20, Jan.-Feb. 2018.

[54] R. W. Going et al., "1.00 (0.88) Tb/s per wave capable coherent multi-channel transmitter (receiver) InP-based PICs with hybrid integrated SiGe electronics," *IEEE J. Quantum Electron.*, vol. 54, no. 4, pp. 1–10, Aug. 2018, Art no. 8000310.

[55] R. Nagarajan et al., "Large-scale photonic integrated circuits," *IEEE J. Sel. Topics Quantum Electron.*, vol. 11, no. 1, pp. 50–65, Jan.-Feb. 2005.

[56] V. Viscardi, D. Schroetter, and M. Kattan, "Routed optical networking: An alternative architecture for IP optical aggregation networks," in *Proc. Int. Conf. Opt. Netw. Des. Model.*, 2022, pp. 1–4.

[57] N. Skorin-Kapov, F. J. M. Muro, M.-V. B. Delgado, and P. P. Marino, "Point-to-multipoint coherent optics for re-thinking the optical transport: Case study in 5G optical metro networks," in *Proc. Int. Conf. Opt. Netw. Des. Model.*, 2021, pp. 1–4.

[58] "OpenZR+ MSA technical specification," Checked on Sep. 29, 2022. [Online]. Available: https://openzrplus.org/

[59] "QSFP-DD/QSFP-DD800/QSFP112 hardware specification," Checked on Sep. 29, 2022. [Online]. Available: http://www.qsfp-dd.com/

[60] "CFP MSA CFP2 hardware specification," Checked on Sep. 29, 2022. [Online]. Available: http://www.cfp-msa.org/

[61] OSFP MSA, "Specification for octal small form factor pluggable module," Checked on Sep. 29, 2022. [Online]. Available: https://osfpmsa.org/

[62] "Implementation agreement for integrated coherent transmit-receive optical sub assembly," Checked on Aug. 20, 2019. [Online]. Available: https://www.oiforum.com/wp-content/uploads/OIF-IC-TROSA-01.0.pdf